

A. De Giacomo · M. Dell'Aglio · A. Casavola ·
G. Colonna · O. De Pascale · M. Capitelli

Elemental chemical analysis of submerged targets by double-pulse laser-induced breakdown spectroscopy

Received: 31 October 2005 / Revised: 16 January 2006 / Accepted: 19 January 2006 / Published online: 17 March 2006
© Springer-Verlag 2006

Abstract Double-pulse laser-induced plasma spectroscopy (DP-LIPS) is applied to submerged targets to investigate its feasibility for elemental analysis. The role of experimental parameters, such as inter-pulse delay and detection time, has been discussed in terms of the dynamics of the laser-induced bubble produced by the first pulse and its confinement effect on the plasma produced by the second laser pulse. The analytical performance of this technique applied to targets in a water environment are discussed. The elemental analysis of submerged copper alloys by DP-LIPS has been compared with conventional (single-pulse) LIBS in air. Theoretical investigation of the plasma dynamics in water bubbles and open air has been performed.

Keywords Laser-induced plasma spectroscopy · Copper alloys · Elemental analysis

Introduction

Laser-induced breakdown spectroscopy (LIBS) consists of detecting the optical emission spectra of a plasma produced by the interaction of a laser beam with the matter. This technique has been widely investigated in the last two decades by the scientific community in connection with different applications of the laser-induced plasmas (LIP) [1]. Several works [2], discussing the potential of LIBS as an analytical tool for in situ determination of the elemental

composition of solid targets, point out its advantages such as the fast response, high sensitivity (generally ppm), the wide range of material that can be investigated without an analytical chamber, the possibility of making the analysis without sampling or surface treatment and the flexibility of the experimental set-up. On the other hand LIBS has also been involved in the characterization of laser-induced plasma processes at low pressure during the production of thin solid films and nano-particles of different materials [3, 4]. From a more classical point of view, the laser plasma emission has been successfully employed for the control of industrial processes and medical applications [5, 6]. These applications have led to a good comprehension of the fundamental questions arising under various experimental conditions and it has been established that the distribution of species in the excited states in the plasma depends on the expanding fluid dynamics of the ablated particles and on the balancing of the elementary processes. Both these aspects have been thoroughly investigated by theory and experiments, and theoretical models can be successfully applied for the interpretation of data in a wide range of conditions [7]. The analytical peculiarities of LIBS and the extent of knowledge developed on laser-induced plasma characteristics clearly suggest the benefits of LIBS methodology for automatization and in situ exploration in difficult environments [8, 9]. In this paper, results obtained by LIBS for the analysis of submerged solid targets are discussed and compared with conventional LIBS analysis in air to investigate the feasibility of this technique for under sea samples where conventional analytical techniques cannot be applied for in situ chemical analysis. Double-pulse LIBS on submerged metallic targets has been investigated by using two different kinds of target: a titanium target for studying the fundamental questions involved in the produced plasma under water, and a set of copper alloy targets to test the analytical capabilities of the technique for submerged samples. To complete the information recovered by experiments, the LIBS technique has also been studied by numerical methods in an attempt to understand some anomalous behaviour observed under particular conditions. Comparison between theoretical and

A. De Giacomo (✉) · A. Casavola · M. Capitelli
Chemistry Department,
University of Bari,
Via Orabona 4,
70126 Bari, Italy
e-mail: alessandro.degiacomo@ba.imip.cnr.it
Tel.: 39-080-5929511
Fax: +39-080-5929501

A. De Giacomo · M. Dell'Aglio · G. Colonna ·
O. De Pascale · M. Capitelli
CNR-IMIP sec Bari,
Via Amendola 122/D,
70126 Bari, Italy

experimental results has been successfully applied to understand the basic phenomenology of double-pulse LIBS underwater, especially when chemical processes are taken into account [10]. The theoretical investigation of the LIBS technique has been applied in different environments (water vapour or air) to support some conclusions of the experimental results.

Experimental

The experimental set-up consists of two doubled Nd:Yag laser sources working at 532 nm, a spectroscopic system, pulse generators and a 500-mL cuvette equipped with lens and target holder, as reported in Fig. 1. The laser sources (Quanta System) provide 7-ns-long pulses with a repetition rate of 10 Hz and variable energy up to 400 mJ at 532 nm. The laser sources are synchronized by a four-channel pulse generator, separately triggering the lamps and the Pockell Cells. The two laser beams are steered along the same direction by using a dichroic mirror. A portion of the beam is deflected by a beam splitter on a fast photodiode to control the inter-pulse delay or to measure the mean energy of the laser beam. The laser beam is focussed on the target surface by a 25-mm-focal-length lens placed directly on the cuvette wall. The target holder rotates at an adjustable distance from the focal point in order to change the fluence on the target surface and at every measurement (30 laser shots) the water in the cuvette is changed. The second laser pulse is the main trigger of the spectroscopic system. It consists of a TRIAX 550 Jobin Yvon monochromator with 1800 gr mm⁻¹ grating, an ICCD i3000 Jobin Yvon unit and a Stanford inc. DG 535 pulse generator for selecting the delay time and the gate width of the detector. The emission light of the plasma is collected by a 7.5-cm-focal-length biconvex lens into an optical fiber or directly on the monochromator slit for spectral resolved imaging. All the receiving optics are in fused silica. When the emission light is collected by the optical fibre the spatial resolution is the fiber core (0.6 mm). When spectral resolved imaging is used the plasma image is focussed directly onto the monochromator slit and a fine alignment of the internal mirrors of the spectrograph is required to placed the image inside the ICCD matrix. Moreover in this case the z axis of the ICCD needs to be calibrated with known distances so that a correspondence between the number of pixels and millimetres can be applied. The laser fluence of the lasers for bubble generation and then plasma production has been set, in agreement with a previous study [10], at 2 and 15 J cm⁻², respectively. The copper alloys certified standard (Tech Lab-Metz-France) has been kindly provided by CNR-IMIP sec Potenza and provides a concentration range of 0.25–6.12% for Pb and 0.26–12.96% for Sn, while the Cu concentration is always higher than 65%. The spectral response of all the detection system and the wavelength calibration has been performed by reference lamps (Spectral Products ASC Series).

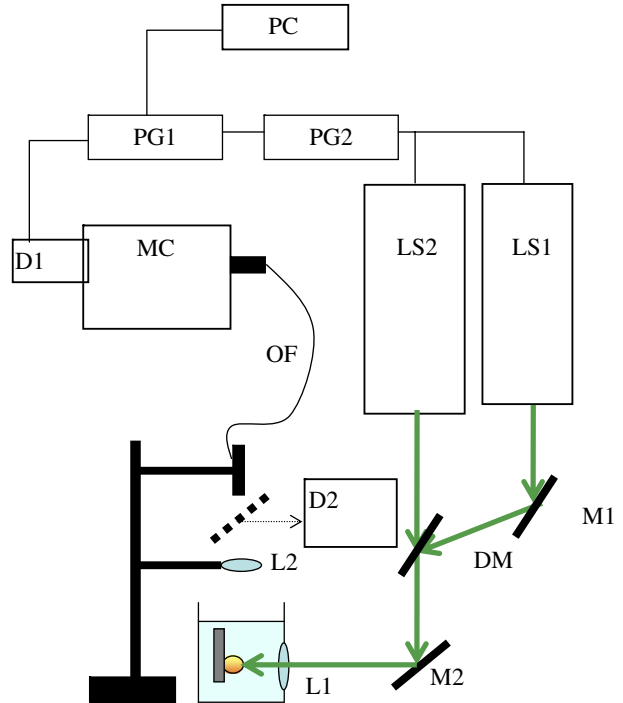


Fig. 1 Experimental set-up: LS_1 and LS_2 are the laser sources for bubble and plasma production, respectively; PG_1 and PG_2 are the pulse generators for synchronizing the laser sources and the detector (D_1); D_2 is the CCD for the imaging; MC is the spectrograph, OF is the optical fiber; M_1 , M_2 , L_1 and DM are mirrors, focussing lens and the dichroic mirror, respectively

Results and discussion

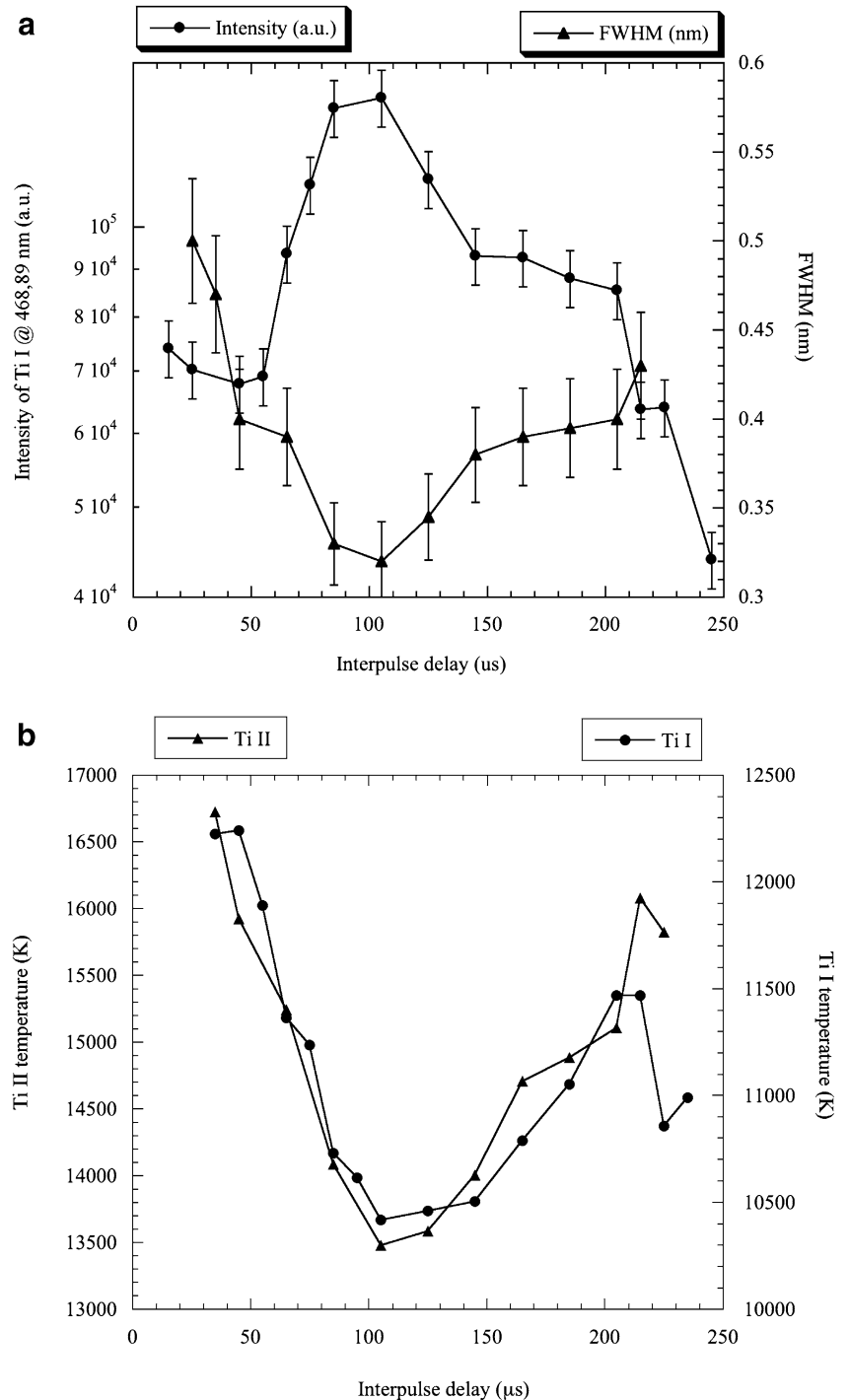
Principles and methods

Single-pulse LIBS experiments in bulk water do not have the adequate accuracy for analytical applications [11, 12]. In this case the laser-induced plasma is rapidly cooled down as its internal energy is suddenly transferred to the surrounding liquid by water vaporization, mechanical effects (sound and vibration) and chemical reactions between the ablated particles and water molecules. For these reasons the optical emission spectrum is characterized by a strong continuum due to the elementary processes connected with free electrons such as Bremsstrahlung processes, especially effective during the laser pulse irradiation, and radiative recombination, which drives a decrease in the density of charged particles after the laser pulse. On the other hand, the spectroscopic emission lines have low intensity and their emission frequencies corresponds to transitions between low energy levels [11]. As a consequence of the plasma energy damping, a bubble develops around the focussed laser spot [10, 13]. The laser-induced bubble, contrary to liquid water, is an appropriate micro-environment where LIBS experiments can be performed; and intense and clear spectra are produced by a second laser pulse when an appropriate time delay is applied [14]. In a previous study [10], it was shown that the laser-induced bubble expands, decreasing the pressure from several tens of atmospheres to 0.8 atm at the

maximum values of the bubble volume and then it collapses, rapidly enhancing its pressure again. In principle, the bubble could pass from different phases of expansion and compression like a damped oscillator, giving its energy to the surrounding water at a slow rate [15]. The bubble oscillation period depends on the laser pulse energy and is of the order of hundreds of microseconds. Therefore, as the bubble is a dynamic system, the choice of the inter-pulse delay is a key parameter to determine the environmental conditions in

which the plasma produced by the second laser pulse expands in. Considering that the emission duration of the plasma obtained by the second pulse in the bubble is less than 5 μ s, it is reasonable to consider the bubble as a quasi-stationary environment, whose conditions depend on the inter-pulse delay time [10, 14]. Figure 2 shows the dependence on inter-pulse delay of line intensity, line broadening and excitation temperature of the plasma obtained by the second pulse during the ablation of a submerged titanium target. In order to detect the entire

Fig. 2 Inter-pulse delay dependence of **a** emission intensity and broadening and **b** excitation temperature of titanium species during double-pulse LIBS under water



lifetime of the plasma in the bubble, the spectra have been collected in time-integrated mode. It is worth noticing that the optimal emission signal is obtained when the second pulse is shot around the time of the maximum expansion of the laser-induced bubble, corresponding, in these experiments, to an inter-pulse delay of 120 μs . Under optimal conditions, the plasma produced by the second laser pulse expands enough to obtain a situation where the dominant processes are the electron-induced excitation and de-excitation collisions leading to emission spectra, whose resolution and intensity are comparable to conventional LIBS in air. When the inter-pulse delay is too short or too long, i.e. during the expansion or collapsing phases of the laser-induced bubble, the plasma expands in a high pressure environment and the spectra are characterized by a strong continuum, while the spectral lines appear broadened by the collision in the confined volume close to the target. The effect of the confinement of the plasma by the background pressure in the bubble is clearly shown by the excitation temperature in Fig. 2b. Here it is shown that the minimum temperature corresponds to the maximum signal as the expansion of the laser-induced plasma allows a longer duration of the spectral lines emissivity.

Due to experimental resolution and sensitivity the description of the plasma dynamics by optical measurements is not complete; however, a theoretical model of the plume expansion can give a more complete characterization of the plasma. The theoretical investigation of the laser-induced plasma is made by solving the time-dependent Euler equations in a one-dimensional approximation [16, 17]. The ablated particles are produced at a constant rate from the surface, while the ambient gas can be water vapour or air. In the case of water we suppose that the plasma and vapour particles cannot exit from the bubble because the particle exchange through the bubble surface is still slower than the bubble dynamics. In contrast, in an air environment an open boundary condition is supposed, because the size of the plasma is smaller than experimental environment. The fluid dynamics equations are coupled with chemical reactions under the hypothesis of local thermodynamic equilibrium [10, 18]. Temperature and pressure values are evaluated after equilibrium calculation to locally preserve mass and energy density. For the system considered in this paper (bronze) the following species are included in the model: Cu, Cu⁺, CuH, CuO, Cu₂, Zn, Zn⁺, ZnH, ZnH⁺, Sn, Sn⁺, SnO, Pb, Pb⁺, PbH, PbO, H₂O, H₂, H₂⁺, O₂, O₂⁺, O₂⁻, H, H⁺, O, O⁻, O⁺, O²⁺, O³⁺, O⁴⁺, OH, OH⁺, OH⁻, N₂, N₂⁺, N₂⁻, N, N⁺, N²⁺, N³⁺, N⁴⁺, NO, NO⁺, e⁻. To simulate the plasma expansion in different environments, two different sets of initial conditions are used, depending on the different background (in air $T_0=50,000$ K, $V_0=10^6 \text{ cm s}^{-1}$, $Z_d=50,000 \text{ kg m}^{-3} \text{ s}^{-1}$; in water $T_0=30,000$ K, $V_0=5\times 10^5 \text{ cm s}^{-1}$, $Z_d=50,000 \text{ kg m}^{-3} \text{ s}^{-1}$) trying to reproduce experimental conditions. In both cases the target is supposed to be evaporated according to stoichiometric coefficients (Cu 88.2%, Zn 0.47%, Sn 9.8%, Pb 0.77%). The background pressure in air and water has been fixed to 1 atm, because the bubble size is almost at its maximum,

obtaining a pressure close to the considered value. The bubble radius is considered to be 5 mm. This value of the bubble radius is larger than the maximum measured in experiments. This choice has been made because the plasma in the water bubble expands approximately in spherical symmetry, and therefore the pressure drops faster than in the one-dimensional case. Considering a larger bubble in the one-dimensional model reduces the pressure at the bubble border to the same level as the experimental values. As a consequence the theoretical results should be considered as a qualitative description of the plume behaviour.

DP-LIBS in water and LIBS in air

The main difference between double-pulse LIBS for a target submerged in water and the traditional single-pulse LIBS for a target in air is the size of the plasma produced. Whereas the interaction between the laser beam and the sample surface should be similar in air and in water bubbles, the differences due to the ambient gas can influence the plume expansion behaviour [1, 9]. Let us discuss the differences between the ablation of a target (titanium or bronze) in air and under water. The expansion in water bubbles is strongly influenced by the bubble size, as discussed above. The emission spectra perform better close to the maximum expansion of the bubble. For this reason we have chosen these conditions for the following considerations.

The first observation concerns the extension and the duration of the LIBS signal: at the same laser fluence (15 J cm^{-2}) the plasma emission in air is detectable for several tens of microseconds and at distances of the order of tens of millimetres, while the corresponding signal obtained in the bubble environment does not exceed the bubble radius (generally a few millimetres) and has a duration shorter than a few microseconds. These results may lead to the wrong conclusion that the plasma produced in the bubble is difficult to detect because excitation temperature and electron number density, the relevant plasma parameters, are low. These considerations are not confirmed by experimental data. Indeed, for the ablation of a titanium target, the measured time-integrated excitation temperature of the plasma in the water bubble is around 14,000 K, whereas it is 8,000 K in air experiments. Moreover, the electron number density measured by time-integrated line broadening in the water bubble is almost one order of magnitude larger than that measured in air. Analogous observations concerning the excitation temperature have been reported in the case of another bronze target [9]. Figure 3 shows the emissivity of a Cu transition ($\lambda=282.44 \text{ nm}$), calculated from particle density and local temperature using the equation [7]

$$I_{ul} = G h \nu_{ul} A_{ul} g_u \cdot \frac{N_A}{Z_A(T_{exc})} \exp(E_u/kT_{exc})$$

as a function of time at three distances from the target (i.e. time of flight, TOF) in water and air. Close to the target (1 mm), the maximum plasma emissivity in water and in air are practically equal. At larger distances (2 mm and 3 mm) the maximum emissivity in water decreases much more than in air. Moreover, the time of flights are larger in water than in air. Another characteristic is that the emission signal appears earlier in air than in water in any considered position. These results can be explained by two considerations. Firstly, the plasma is more confined in water than in air; secondly, in air it moves faster than in water.

These results suggest that an important role is played by the environment in which the plasma expands and two main reasons can be outlined: (a) different plasma dynamics occur as a consequence of the confinement due to the bubble; (b) the ambient gas (water or air) reacts differently with particles of the plasma plume.

The main effect on the emission spectra is that LIBS signal (space integrated) has shorter duration (a) and the oxides of the plasma atoms, produced by the interaction of the plume with the surrounding gas, appear at shorter times in water bubble than in air (b). Figure 4 shows the temporal evolution of the experimental LIP spectrum in the region of TiO molecular bands obtained by double-pulse LIBS in water and the appearance of a TiO emission band it is notable from the beginning of the plasma expansion. The same band appears in air, with comparable intensity, at a time delay greater than 30 μ s [19]. The same characteristic should be evident when LIBS is applied to the bronze target. Unfortunately, the emission bands of CuO between 600 and 640 nm are weak and have not been detected during these experiments. For this reason, the spatial profile of CuO in water and in air has been reported in

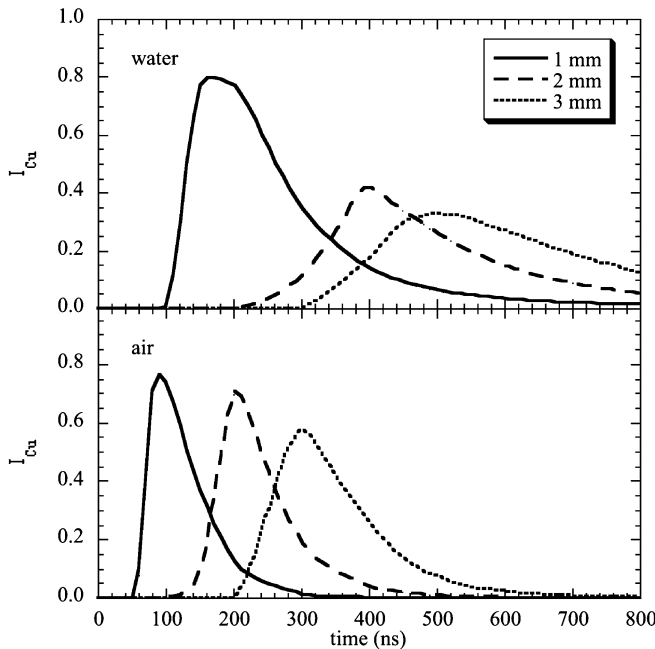


Fig. 3 Calculated Cu emission time of flight at 1, 2 and 3 mm from the target for LIBS in air and in water

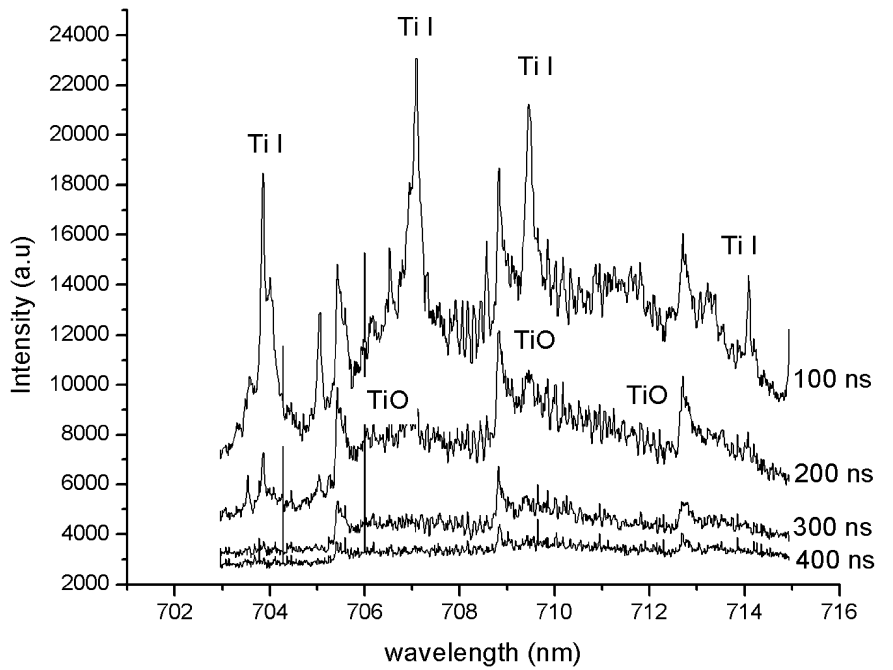
Fig. 5 at different times as obtained by theoretical calculation for a bronze target. The CuO molecules appear in water closer to the target than in air and the concentration is larger in water than in air. Moreover, the CuO molarity in air increases as the plasma moves farther from the target due to the expansion cooling. These results suggest that the emitting plasma inside the bubble is strongly confined in a small volume leading to spectra characterized by a better thermalization with the electron gas. In contrast, during LIBS experiments in air, the emitting volume of the plasma comprising the contribution from the hot core and of the colder wings due to the different expansion modes (longitudinal and radial) of species. The average values of excitation temperature and electron number density obtained by spectroscopic measurements are smaller than the corresponding one in water bubble, where the cold part at the plasma boundary has a negligible contribution due to disappearance of the plasma species in reactions with water molecules (see also Fig. 3: the decreasing of the plasma emission in water is due mainly to the plasma damping, whereas in air it is due to the shift in space of the maximum emissivity). Moreover, the increasing pressure inside the bubble during the plasma expansion further enhances the reaction rate as a consequence of the increasing of the reactants concentration.

Figure 6 shows the experimental temporal displacement of the maximum of the optical time of flight (O-TOF) of Cu, Sn, and Pb during double-pulse LIBS on a submerged copper alloy target. The reported results show that the plasma emission is rapidly slowed down by the pressure inside the bubble and by emission decreasing due to the interaction of plasma species with the surrounding water particles.

A direct confirmation of the plasma confinement in water can be observed in Fig. 7, where the calculated water bubble pressure-time profiles are compared with the results calculated in air. For $t=100$ ns the pressure profiles in water and air are very close to each other even if the pressure in the bubble is higher than in air. For $t=400$ ns the maximum of the pressure in the bubble is diminished and is positioned around 2.2 mm from the target, and for $t=800$ ns a strong increase of the pressure at the bubble border means that the plasma expansion is blocked. Comparing with Fig. 3, we can also assert that the plasma has been partially depleted. On the other hand, in the air environment, the maximum of the pressure seems to travel undisturbed and its temperature decreases due to the expansion, as confirmed by Fig. 3 (small decrease of the emissivity) and Fig. 4 (increase of CuO concentration).

We must point out that the depletion of the plasma observed for calculations in the water environment is due only to interaction with the vapour in the bubble because water evaporation and mechanical energy loss have been neglected.

Fig. 4 Emission spectra at different delay times during double-pulse LIBS under water in the region of TiO molecular band



Analytical performance

To investigate the analytical performances of DP-LIBS in a water environment, we have detected the emission lines of Sn at 284.00 nm, Pb at 283.31 nm and Cu at 282.44 nm for eleven standards of copper alloys. It is well known that LIBS analysis of copper alloys in air is not accurate because of target fractionation [20], so that the concentration of species in the plasma does not reproduce sample composition. In order to find the optimal temporal acquisition parameters, spectral resolved imaging has

been performed with a delay time step of 100 ns. Spectral resolved imaging allows one to investigate the central slice of the plasma along the propagation direction because each row of pixels corresponds to a space interval, whereas each column corresponds to a specific wavelength. A typical spectral resolved image is shown in Fig. 8. To find an appropriate temporal window in which the plasma stoichiometry is homogeneous the ratio of Sn, Pb and Cu lines has been investigated for each array of the ICCD matrix. It has been found that, excluding the first 100 ns from the laser pulse where the continuum emission is dominant, the plasma holds a good stoichiometric composition in all the emitting region until 300 ns and then the emission line

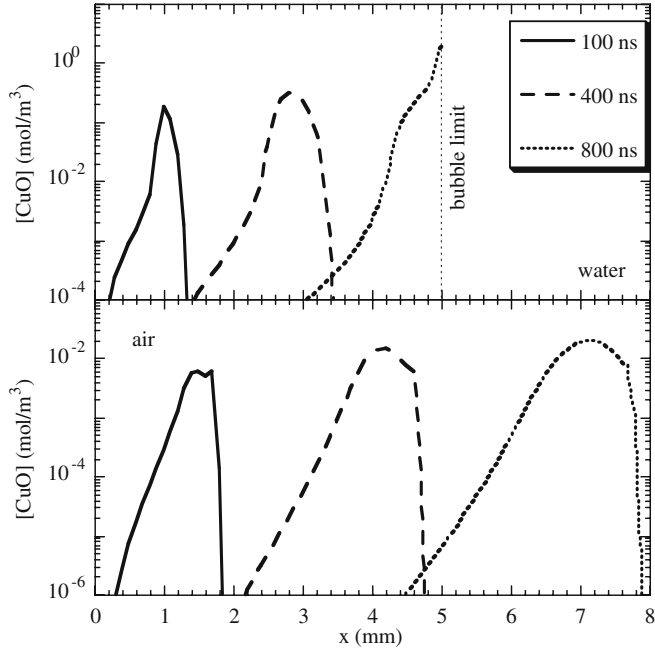


Fig. 5 Calculated spatial concentration distribution of CuO species at different times during LIBS in air and in water

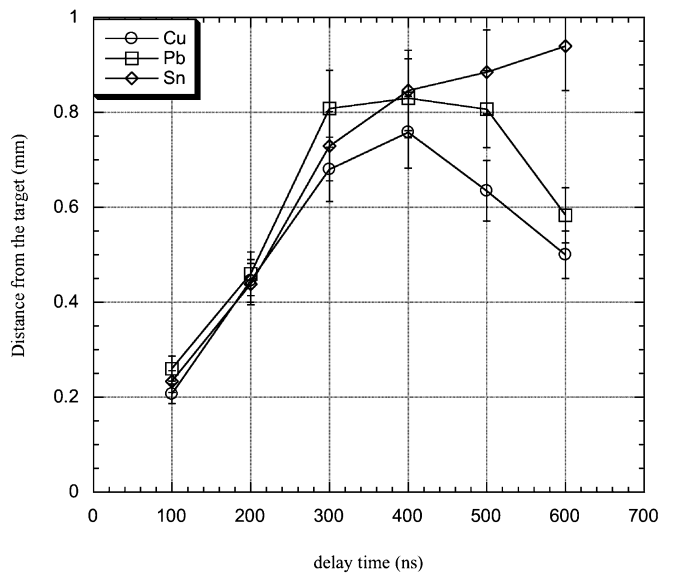


Fig. 6 Displacement as function of time of the maximum of the spatial distribution of Cu I, Pb I and Sn I species as obtained by spectral resolved imaging

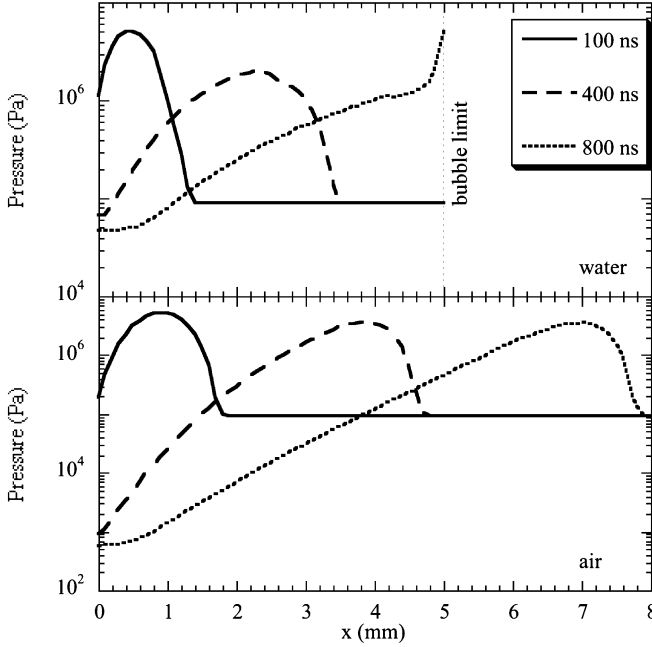


Fig. 7 Calculated spatial pressure distribution at different times in air and in water

distribution starts to differ along the propagation direction as shown in Fig. 6. As mentioned in the previous section, this is probably due to the different reaction rate of the investigated elements with water molecules inside the bubble. Fortunately, as shown in Fig. 9, the prevailing contribution to the integrated time emission signal is that

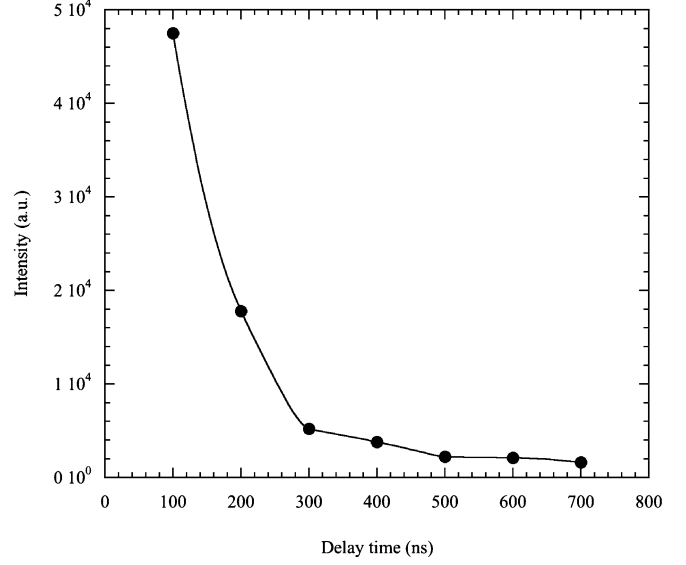


Fig. 9 Temporal evolution of the emission intensity of Cu I line at 282.31 nm obtained by spectral resolved imaging

detected in the first 300 ns, so that it is possible to perform the analysis even without time gating of the detector, because the contribution of the temporal window where the plasma is dishomogeneous is almost one order of magnitude less intense.

The selected lines for quantitative analysis are shown in the spectrum reported in Fig. 8 and it can be observed that a Cu II line at 288.42 has been analysed, too. The ratio of Cu II and Cu I lines has been used for checking that the

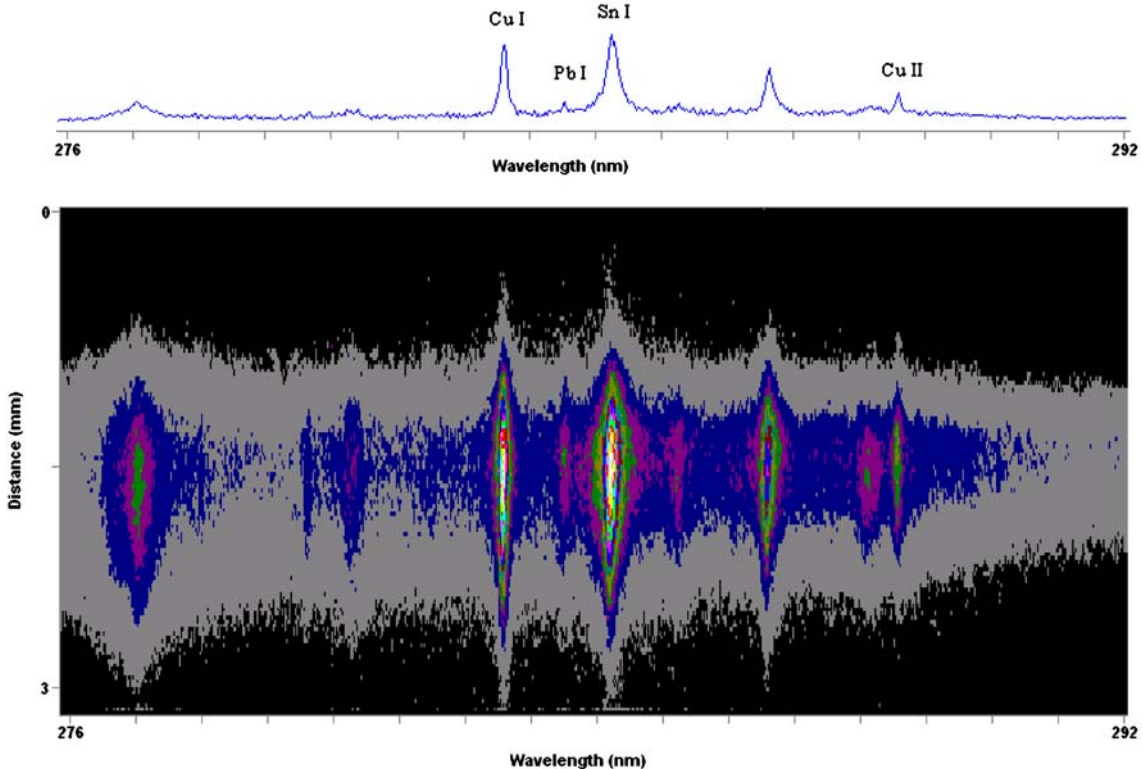


Fig. 8 Example of a spectral resolved imaging detection of the investigated spectral region

investigated plasma, obtained by each standard, is in the same thermodynamic condition, since the ratio is proportional to the ionization degree of the major constituent of the investigated alloys [14].

The calibration curves obtained by double-pulse LIBS under water are reported in Fig. 10 together with those obtained by the same experimental set-up, but with a gated detector, with conventional LIBS in air. All the calibration curves have been obtained by adopting Cu I at 282.44 nm as internal standard. In Table 1 the limit of detection (LOD) and the slope and the correlation factor of the calibration curve are reported for measurements made in air and by double-pulse LIBS in water, respectively, for Sn and Pb. The LOD has been calculated by the following formula:

$$\text{LOD} = 3\sigma/s,$$

where σ is the standard deviation of the background of the experimental spectrum and s is the calibration curve slope. From Table 1 it is notable that whereas the correlation coefficient, R , of the curve is comparable in the water bubble and in air, the variation of intensity as function of analytics concentration is higher, suggesting a better accuracy in the elemental composition determination in agreement with what was observed in previous work [10, 14].

Conclusions

In this work double-pulse LIBS on submerged targets has been discussed from an analytical point of view. The effect of the laser-induced bubble produced by the first pulse, in order to obtain an appropriate environment in which to perform the LIBS experiment, has been discussed from both the experimental and theoretical points of view. The confinement due to the presence of the bubble has been observed experimentally and predicted by calculations. The comparison of conventional LIBS in air and double-pulse LIBS on submerged targets has been performed to investigate the effects of different expansion environments.

Table 1 Comparisons between analytical performances of conventional LIBS (4 μ s gated) in air and Double Pulse LIBS in water: the columns report the experimental background environment, the correlation coefficient ($R\%$) and the slope of the calibration curves and the low detection limit (LOD) respectively

Environment	$R\%$	Slope	LOD (%w)
Sn I @ 284.00 nm			
LIBS in air	99.4	0.142	0.05
DP-LIBS in water	99.4	0.236	0.03
Pb I @ 283.31 nm			
LIBS in air	94.1	0.072	0.09
DP-LIBS in water	97.0	0.079	0.08

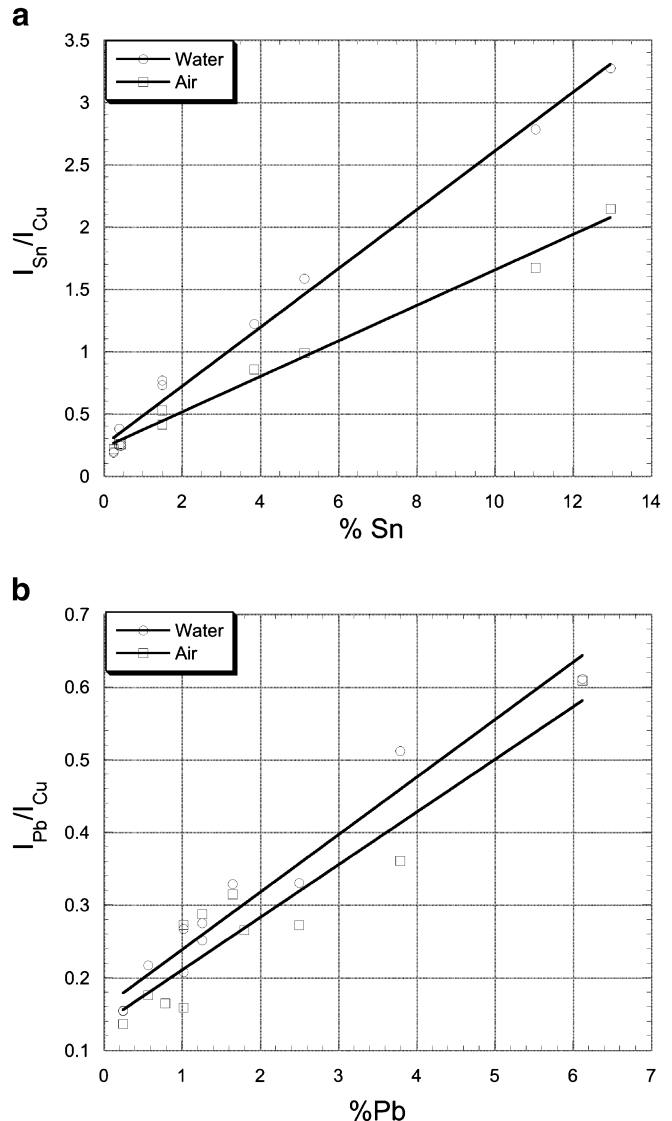


Fig. 10 LIBS calibration curves of Sn and Pb in air and by double-pulse LIBS in water (120 μ s of inter-pulse delay, 30 accumulations). The concentration is expressed as a percentage of weight

The strong confinement of the bubble enhances the emission optical signal of the ablated material making DP-LIBS feasible as an underwater, in situ, analytical technique. The accuracy of the technique for underwater analysis has been demonstrated by the calibration curve of copper alloy samples. Theoretical calculations, with the aid of experimental results, can be a useful tool to obtain a detailed description of the plume dynamics of laser-induced plasmas.

Acknowledgements This work has been supported by MIUR PON TECSIS and FIRB 2001-RBAU01H8FW-03 Dinamica Microscopica delle Reattività Chimiche.

References

1. LJ Radziemski, DA Cremers (eds) (1989) Laser-induced plasma and applications. Marcel Dekker, New York
2. WB Lee, J Wu, Y Lee, J Sneddon (2004) *Appl Spectrosc Rev* 39/1:27–97
3. A De Giacomo, VA Shakhmatov, GS Senesi, S Orlando (2001) *Spectrochim Acta B* 56:1459–1472
4. SRJ Pearce, SJ Henley, F Claeysseens, PW May, KR Hallam, JA Smith, KN Rosser (2004) *Diamonds Relat Mater* 13:661–665
5. R Noll, H Bette, A Brysch, M Kraushaar, I Monch, L Peter, V Sturm (2001) *Spectrochim Acta B* 56:637–649
6. PK Kennedy, DX Hammer, BA Rockwell (1997) Laser induced plasma in aqueous media. *Prog Quant Electr* 21(3):155–248
7. M Capitelli, A Casavola, G Colonna, A De Giacomo (2004) *Spectrochim Acta Part B* 59:271–289
8. L Radziemski, DA Cremers, K Benelli, C Khoo, RD Harris (2005) *Spectrochim Acta Part B* 60:237–248
9. A De Giacomo, M Dell'Aglio, F Colao, R Fantoni, V Lazic (2005) *Appl Surf Sci* 247/1–4:157–162
10. A Casavola, A De Giacomo, M Dell'Aglio, F Taccogna, G Colonna, O De Pascale, S Longo (2005) *Spectrochim Acta Part B* 60:975–985
11. A De Giacomo, M Dell'Aglio, O De Pascale (2004) *Appl Phys A* 79:1035–1038
12. S Koch, W Garen, M Muller, W Neu (2004) *Appl Phys A* 79:1071–1073
13. AE Pichahchy, DA Cremers, MJ Ferris (1997) *Spectrochim Acta Part B* 52:25–39
14. A De Giacomo, M Dell'Aglio, F Colao, R Fantoni (2004) *Spectrochim Acta Part B* 59/9:1431–1438
15. CE Brennen (1995) Cavitation and bubble dynamics, Oxford University Press
16. A Casavola, G Colonna, A De Giacomo, M Capitelli (2003) *J Thermophys Heat Transf* 17(2):225–231
17. A Casavola, G Colonna, A De Giacomo, M Capitelli (2004) *Appl Phys A* 79:1315–1317
18. G Colonna, A Casavola, M Capitelli (2001) *Spectrochim Acta Part B* 56:567–586
19. A De Giacomo, M Dell'Aglio, A Santagata, R Teghil (2005) *Spectrochim Acta Part B* 60:935–947
20. V Margetic, A Pakulev, A Stockhaus, M Bolshov, K Niemax, R Hergenroder (2000) *Spectrochim Acta Part B* 55:1771–1785